FEA Information International News
For The
World-Wide Engineering Community

STRELA - Russia

hp invent

eta

The Japan Research Institute, Limited

EASi

ANSYS

Oasys

LSTC

sgi

FUJITSU

LMS INTERNATIONAL
Empowering Engineering Innovation

MSC SOFTWARE
SIMULATING REALITY

December 19, 2001

FEA Information Inc.
www.feainformation.com

Featured Articles

FEA Information Inc. ONLY uses the following e-mail addresses
vic@lstc.com
feainfo@lstc.com

FEA Information Inc. welcomes a new sponsor:
ANSYS CHINA

Part 4
Airbag Contact, Edge-to-Edge Contact, and Rigid Body Contact
Figures are located on the last page of this article

8.0   Airbag Contact

Simulation of airbag deployment and interaction of an airbag with other components may require special contact treatment. Some of the challenges associated with airbag contact are as follows:

- High Airbag Nodal Velocity (> 100 m/s)
- Soft Tissue Properties (E < 50 Mpa)
- Small Tissue Thickness (< 0.5 mm)
- Frequent Initial Penetrations in Folded Bag
- Treatment of Airbag Fabric Layers

To promote stability and accuracy in simulating airbag contact, the following contact types and contact parameters are recommended.

8.1   Airbag Self-Contact

When treating airbag self-contact (fabric-to-fabric contact), the use of *CONTACT_AIRBAG_SINGLE_SURFACE is highly recommended. This contact type is based on *CONTACT_AUTOMATIC_SINGLE_SURFACE but has significant modifications to account for the difficulties associated with deployment of a folded airbag.

SOFT=2 is generally recommended (SMP only) to better deal with the many initial penetrations present in a folded airbag and to invoke a segment-to-segment contact search which is often advantageous in dealing with the complex geometry of a folded or partially unfolded airbag. Airbag contact with SOFT=2 is expensive relative to other contact options so to improve cpu performance when using SOFT=2, an additional contact with SOFT=0 or1 can be implemented as shown in Figure 8.1. By defining two separate contacts and employing contact birthtime and deathtime to switch from the SOFT=2 contact to the SOFT=1 contact when the bag has unfolded, a good combination of contact reliability and efficiency can be acheived.

If the airbag simulation is run using an MPP executable, note that SOFT=2 is not yet available and so SOFT=0 or 1 must be used. For a folded airbag, this will likely mean that a load curve defining the fabric contact thickness versus time will be necessary to transition from a very small thickness in the folded state to a larger thickness as the bag unfolds. This is done to prevent initial penetrations in the folded state and still have good contact behavior during the unfolding process. The contact thickness vs. time curve is identified by LCIDAB on Optional Card A of *CONTACT. As a possible alternative to a time-dependent contact thickness, the user may try invoking the option for tracking of initial penetrations by setting IGNORE=1 on Optional Card C. This latter option is new in version 960 and has not been thoroughly checked out for airbag applications.

8.2   Airbag-to-Structure Contact

During and after airbag deployment, the airbag fabric comes into contact with other parts of the model such as the steering wheel, occupant, instrument panel, door trim components and, in the case of side curtain

deployment, the seat. For these contact conditions, a two-way contact such as *CONTACT_AUTOMATIC_SURFACE_TO_SURFACE is generally recommended. In instances when the airbag nodes comprise the slave side in a one-way type contact such as *CONTACT_AUTOMATIC_NODES_TO_SURFACE, the structural nodes are not checked for penetration through the airbag segments. This may result in noticeable penetration of finely-meshed structural components into airbag segments. Single surface contacts such as *CONTACT_AUTOMATIC_SINGLE_SURFACE for airbag-to-structure interaction may be ill-advised as this would result in duplication of self-contact treatment for the fabric.

Difficulties in airbag-to-structure contact are largely associated with significant differences in material bulk moduli (up to 1000x) and very low thickness of the fabric. To avoid premature nodal release triggered by a small fabric thickness, it is recommended that the contact thickness of the fabric be set to a minimum value of 1.0 mm. Since a wide range of materials are involved, the use of SOFT=1 is highly recommended as it eliminates the need to fine-tune penalty scale factors.   An example of the overall setup for airbag-related contact is shown in Figure 8.2.

9.0   Edge-to-Edge Contact

Most contact types do not check for edge-to-edge penetrations as the search entails only nodal penetration through a segment. This may be adequate in many cases; however, in some unique shell contact conditions, the treatment of edge-to-edge contact becomes very important. There are several ways to handle edge-to-edge contact; the merits/demerits of each one of these methods are discussed below.

9.1   *CONTACT_AUTOMATIC_GENERAL excluding Interior Edges

By default, *CONTACT_AUTOMATIC_GENERAL considers only exterior edges in its edge-to-edge treatment as indicated by Figure 9.1. An exterior edge is defined as belonging to only a single element or segment whereas interior edges are shared by two or more elements or segments. The entire length of each exterior edge, as opposed to only the nodes along the edge, is checked for contact. As with other penalty-based contact types, SOFT=1 can be activated to effectively treat contact of dissimilar materials.

9.2   *CONTACT_AUTOMATIC_GENERAL including Interior Edges

Edge-to-edge contact which *includes* consideration of interior edges may be invoked in one of two ways. One method takes advantage of the beam-to-beam contact capability of *CONTACT_AUTOMATIC_GENERAL. This labor-intensive approach involves creating null beam elements (*ELEMENT_BEAM, *MAT_NULL) approximately 1 mm in diameter (elform=1, ts1=ts2=1,2mm, tt1=tt2=0 in *SECTION_BEAM) along every interior edge wished to be considered for edge-to-edge contact and including these null beams in a separate AUTOMATIC_GENERAL contact. This is illustrated in Figure 9.2. The elastic constants in *MAT_NULL are used in determining the contact stiffness so reasonable values should be given. Null beams do *not* provide any structural stiffness.

A preferred alternative to the null beam approach, available in version 960, is to invoke the interior edge option by using *CONTACT_AUTOMATIC_GENERAL_INTERIOR. A certain cost penalty is associated with this option.

9.3   *CONTACT_SINGLE_EDGE

This contact type treats edge-to-edge contact but, unlike the other options above, it treats *only* edge-to-edge contact. This contact type is defined via a part ID, part set ID, or a node set on the slave side. The master side is omitted.

4

10 Rigid Body Contact

Components for which deformation is negligible and stress is unimportant may be modeled as rigid bodies using *MAT_RIGID or *CONSTRAINED_NODAL_RIGID_BODY. The elastic constants defined in *MAT_RIGID are used for contact stiffness calculations. Thus the constants should be reasonable (properties of steel are often used).

Though there are several contact types in LS-DYNA which are applicable specifically to rigid bodies (RIGID appears in the contact name), these types are seldom used. Any of the penalty-based contacts applicable to deformable bodies may also be used with rigid bodies, and in fact, are generally preferred over the RIGID contact types. Rigid bodies and deformable materials may be included in the same penalty-based contact definition. Constraints and constraint-based contacts may not be used for rigid bodies.

Rigid bodies should have a reasonably fine mesh so as to capture the true geometry of the rigid part. An overly coarse mesh may result in contact instability. Another meshing guideline is that the node spacing on the contact surface of a rigid body should be no coarser than the mesh of any deformable part which comes into contact with the rigid body. This promotes proper distribution of contact forces. As there are no stress or strain calculations for a rigid body, mesh refinement of a rigid body has little effect on cpu requirements. In short, the user should not try to economize in the meshing of rigid bodies.

*CONTACT_ENTITY is an altogether different way of defining an analytic, rigid contact surface which interacts with nodes of deformable bodies. For more information

Red. SOFT=2

Blue. SOFT=0.1

On

Off

20-30 ms into deployment,

Simulation Time,
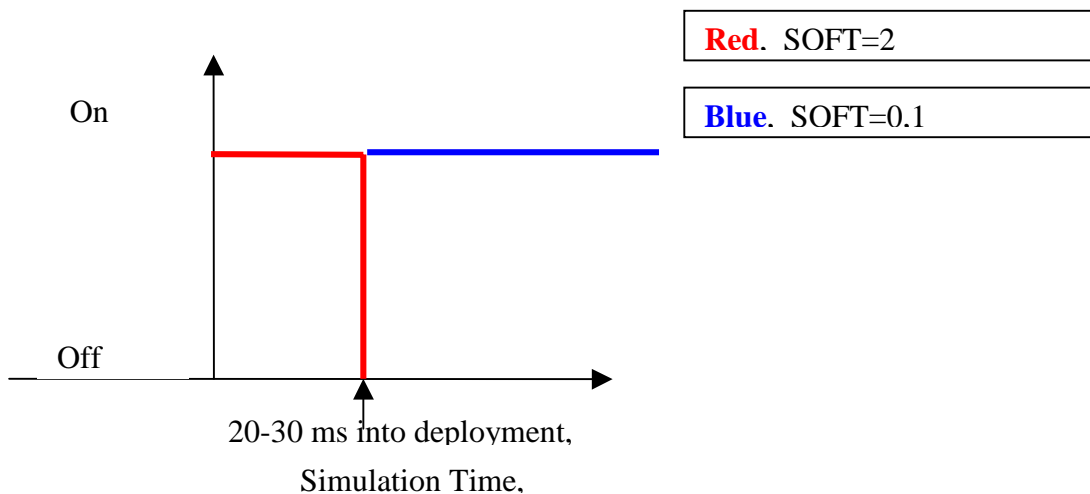
Figure 8.1   Airbag Self Contact Algorithm Switch

5

Structural Contact,
*CONTACT_AUTOMATIC_SURFACE_TO_SURFACE,
SOFT=1,SST=1.0, fabric(slave-material)

Self Contact,
*CONTACT_AIRBAG_SINGLE_SURFACE
SOFT=2
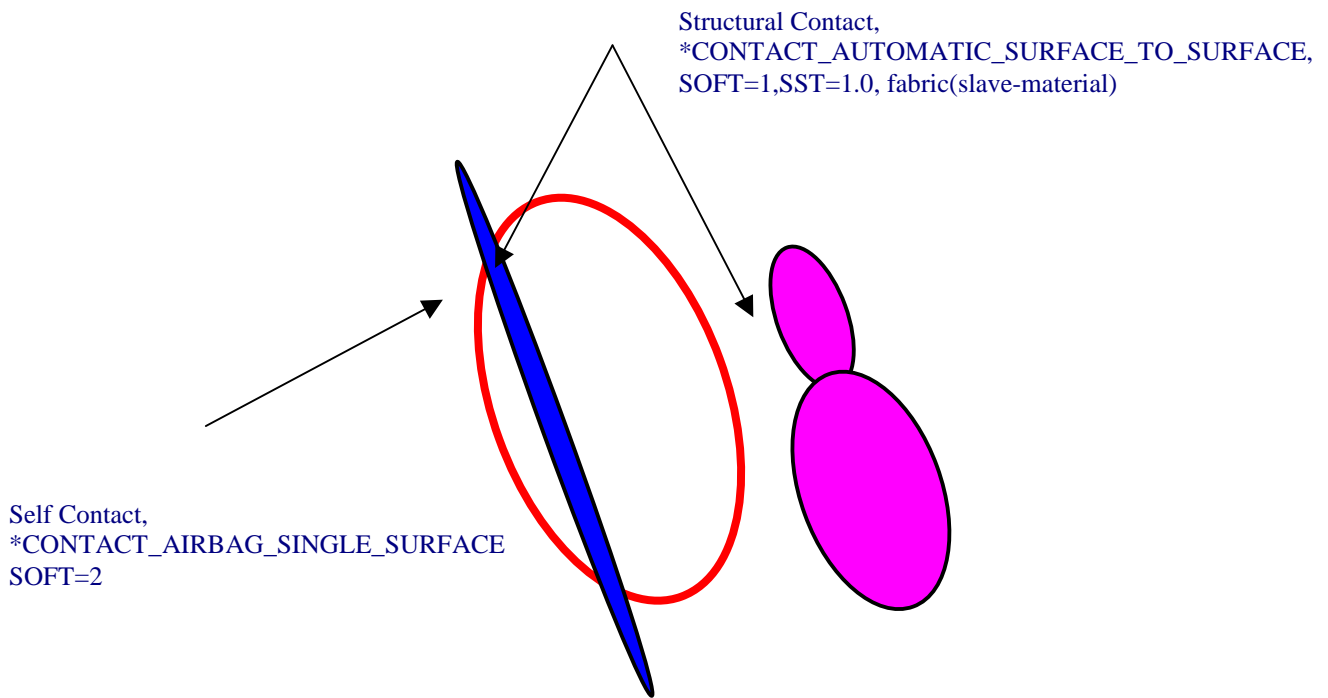
Figure 8.2   Airbag Contact Definition
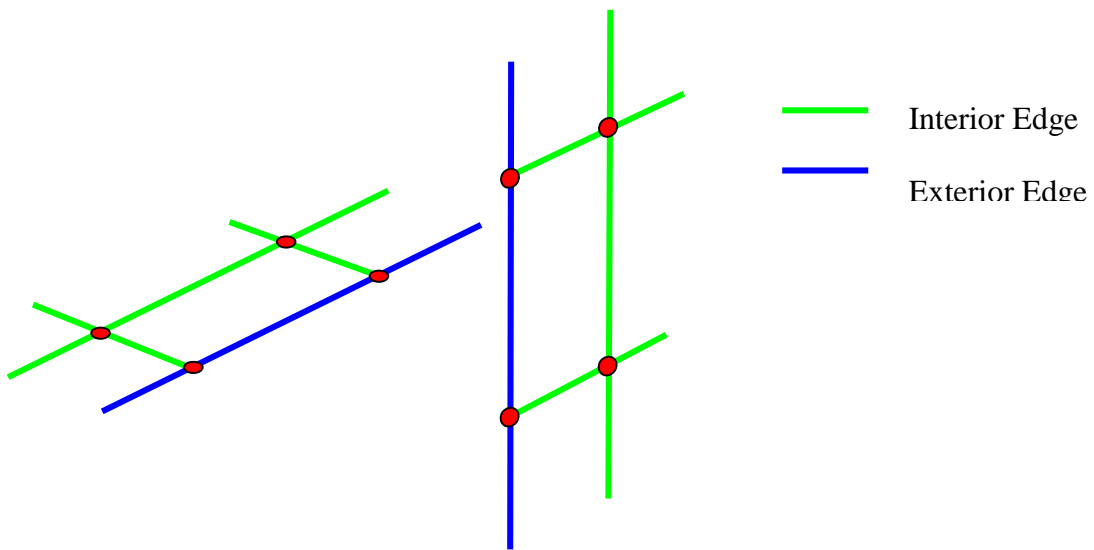
Figure 9.1   Interior and Exterior Shell Edges
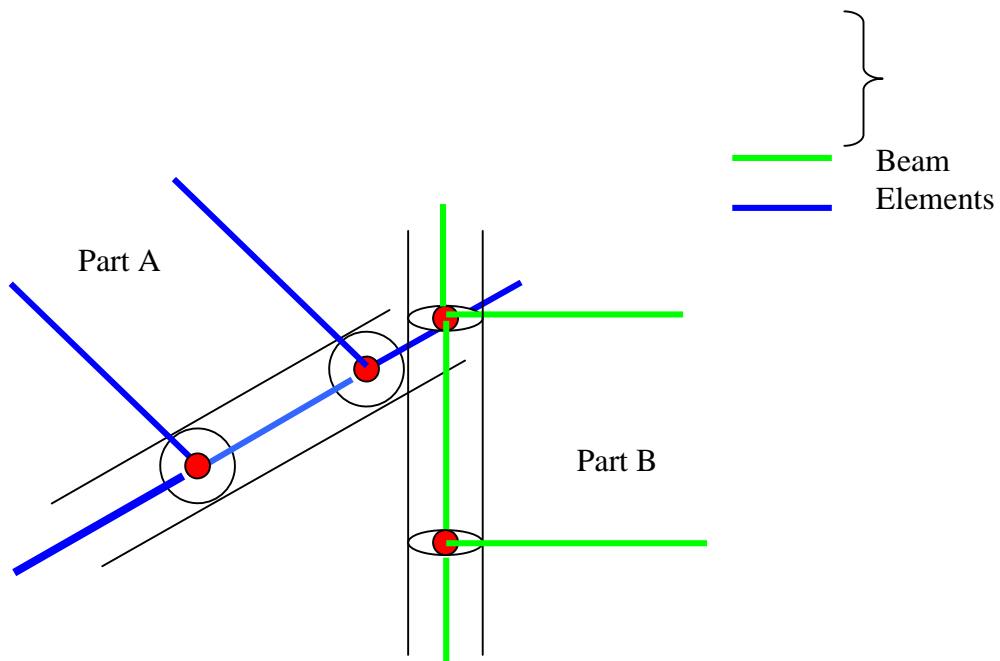
Figure 9.2   Null Beams to treat edge-to-edge treatment

Laboratory Tests for Characterizing Geomaterials
Len Schwer - Len@Schwer.net
December 2001

Bold – Sections Introduced in this article
The Complete Article can be found on the web site Geomaterial Modeling
www.geomaterialmodeling.com

Introduction

Engineering analysts are familiar with the uniaxial stress test used to characterize most metals, and used to calibrate the parameters associated with metal plasticity material models. However when the need arises to model geomaterials (concrete, rock, and soil), and some simple foams, the same analysts may be unfamiliar with the required suite of material characterization tests needed for calibrating the material model parameters in appropriate geomaterial constitutive models.

In this brief article a description of three common laboratory geomaterial tests are presented along with the corresponding material model parameters that are characterized by these tests. The tests covered are:
1. Hydrostatic compression
2. Triaxial compression/extension
3. Uniaxial strain

The material model parameters that can be calibrated to this data are used in the following LS-DYNA constitutive models:
- Soil and Foam (Material Type 5)
- Pseudo TENSOR (Material Type 16)
- Geologic Cap Model (Material Type 25)

Laboratory Test Specimens

The typical geomaterial laboratory test specimen is a right circular cylinder. For concrete the standard (United States) specimen has a 6 inch (152 mm) diameter and 12 inch (305 mm) height and is tested 28 days after the concrete is poured. More commonly, laboratory specimens have a 2 inch (51 mm) diameter and 4 inch (101 mm) height.

The cylinders are tested by applying axial and lateral loads (stresses) and recording the corresponding axial and lateral displacements (strains). The geometry of the cylinders, and applied loads, provides for an axisymmetric state of stress, and strain, in the cylinders that is typically denoted by the two principal stress components σ_1 and σ_3, where σ_1 is the stress applied in the axial direction and σ_3 is the lateral, or confining, stress applied to the cylindrical surface, see Figure 1. Note: the other principal stress, σ_2, by symmetry, is equal to the confining stress, i.e. $\sigma_2 = \sigma_3$.
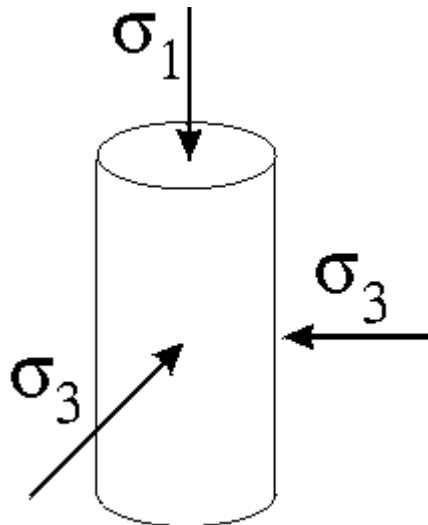
Figure 1 Typical geomaterial cylindrical laboratory specimen and axisymmetric loading.

Laboratory Tests

Figure 2 shows a schematic of the stress trajectories for five of the most common types of geomaterial characterization tests. Each of these five tests are briefly described in the sections that follow. After describing the tests, a summary of the geomaterial model parameters, for three LS-DYNA geomaterial constitutive models, is presented with an associated test to be used to calibrate each input parameter.
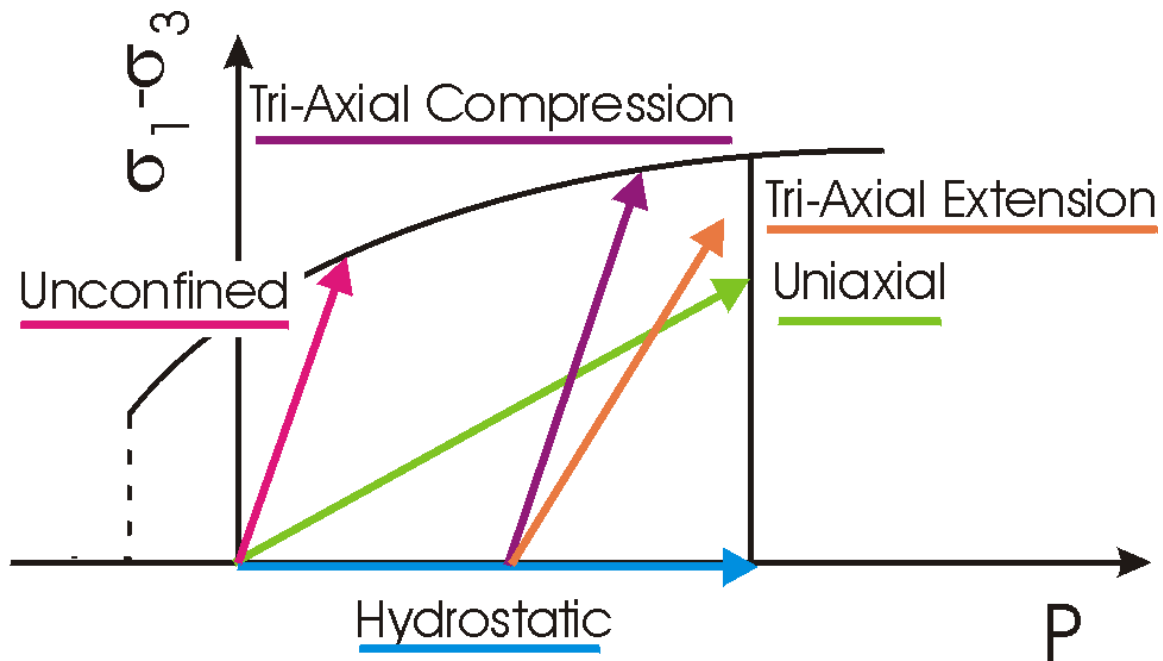
Figure 2 Stress trajectories for material characterization.

Hydrostatic Compression Tests

When the axial and lateral stresses are equal

$$\sigma_1 = \sigma_3 = \sigma$$

the specimen is in a state of hydrostatic compress (HSC) with a pressure

$$p = \sigma_{kk}/3 = (\sigma_1 + 2\sigma_3)/3 = \sigma$$

The corresponding measured axial and lateral strain components provide the volume strain

$$\varepsilon_v = \varepsilon_{kk} = (\varepsilon_1 + 2\varepsilon_3)$$

The corresponding pressure versus volume strain response describes the compaction behavior of the material as shown schematically in Figure 3. A typical geomaterial compaction response has three phases:
1. $p_0 < p < p_1$ is the initial elastic response. The elastic ***bulk modulus***, K, is the slope of this segment.
2. $p_1 < p < p_2$ is when the pores (voids) in the material are compressed,

3. $p > p_2$ removal of the voids results in a fully compacted material.

The indicated fourth phase is the unloaded from the fully compacted state. The slope of this segment defines the **bulk unloading modulus**, K_{un}, which is a user input for the Soil & Foam model (Material Type 5). Note the bulk unloading modulus should always be greater than the elastic modulus to prevent fictitious generation of energy during loading-unloading cycles.

It is important to note that, in general, LS-DYNA expects strain to be input as logarithmic strains. In the case of the volume strain, the measured (engineering) volume strain is related to the logarithmic volume strain by the simple relation

$$\ln \frac{V}{V_0} = \ln\left(1 - \varepsilon_{kk}\right)$$

If the measured volume strains are great than about 10%, the conversion becomes important.
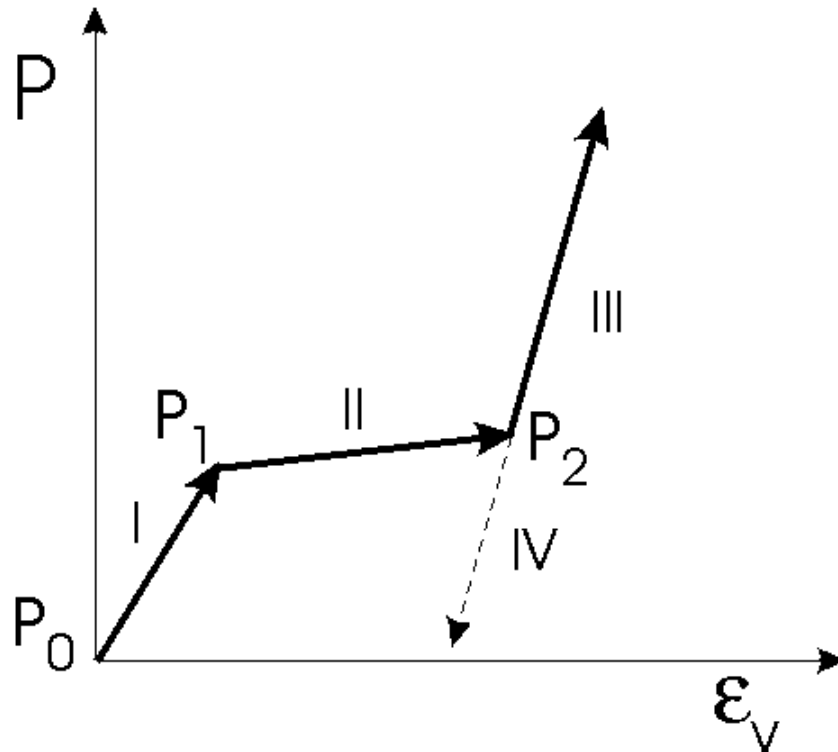
Figure 3 Schematic of pressure versus volume (compaction) response for a geomaterial.

Aspects of Shell Element Technology

Sections:
2.1 : introduction
2.2 : common features of shell elements in LS-DYNA

2.1 : Introduction :

- **Current shell element formulations in LS-DYNA : (version 940)**

Type	Name	Nodes	Interpolation Order	cpu
1	**Hughes-Liu**	4	2	3.5
11	Fast Hughes-Liu	4	2	
6	SRI Hughes-Liu	4	2	20.
7	Fast SRI Hughes-Liu	4	2	10.
2	Belytschko-Lin-Tsay	4	2	1.
10	Belytschko-Wong-Chiang	4	2	1.1
8	Belytschko-Leviathan	4	2	1.3
3	Belytschko-Machertas	3	3	
4	Belytschko-Kennedy	3	2	
5	membrane	4	2	
9	FI membrane	4	2	
16	FI-ANS (Bathe-Dvorkin)	4	2	3.5

The Hughes-Liu element family were the first shell elements to be implemented in LS-DYNA

The table shows the remarkable efficiency of the Belytschko-Tsay element compared to fully integrated shells

An additional advantage of this element for crashworthiness analysis is the numerical robustness of the formulation (warp angles of 180 degrees usually do not cause coredumps)

Consequently the BT element is the workhorse of all crashworthiness analysis

2.2 : Common features of shell elements in LS-DYNA:

Almost all shell formulations in LS-DYNA are lower order elements using bilinear interpolation functions to define the element surface from the nodal coordinates. (Type 3 is the only exception)

User Input

Finite Element Surface

4 Nodal Points :

N1 (x1,y1,z1)
N2 (x2,y2,z2)
N3 (x3,y3,z3)
N4 (x4,y4,z4)
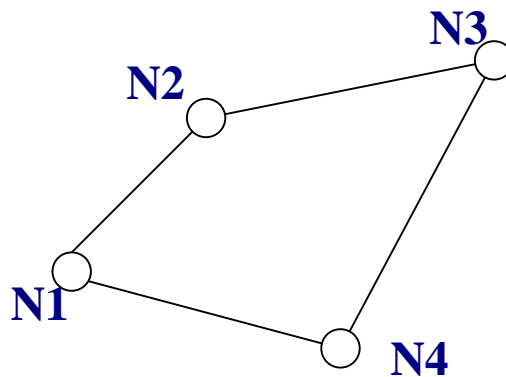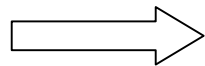
Bilinear interpollation creates an element surface where all 4 edges are straight lines, the element surface is flat if the 4 nodes are coplanar.

These lower order elements are preferred because of :
- simplicity of coding
- numerical robustness
- higher order elements lead to reduced timestep values
  in explicit codes

Shell element formulations with bilinear interpolation

The real curved CAD-surface is approximated by a finite number of element surfaces (the FE-surface) interpolated bilinearly between the nodal point locations : (with flat elements we obtain a polygonal surface) :
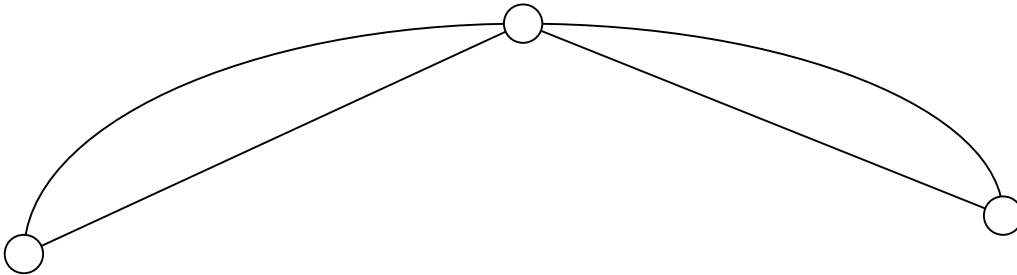
Available elements are :
* 3-node shells (type 4)
* flat & warped 4-node shells (types 1-2-6-7-8-10-11-16)

The element surfaces represent the midplane of the shell, except if an offset is defined (only types 1-6-7-11)

We approximate a curved CAD-surface by a polygonal FE-surface, even if all nodal points are on the CAD-surface.

Smooth curved surfaces are thus approximated by surfaces with kinks (element angles).

A smooth undeformed finite element surface will develop kinks during bending deformation.

Element angle
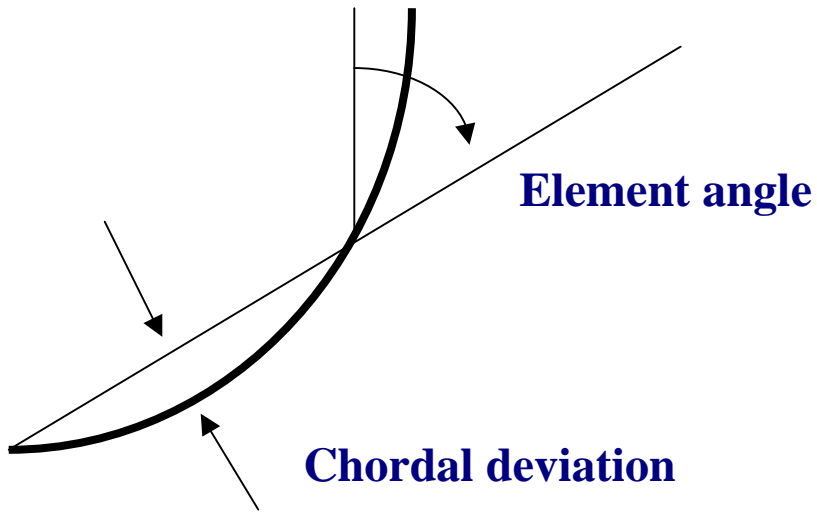
Chordal deviation

Mesh refinement is the only way to reduce kinks and chordal deviation !

Bilinear Interpolation:

We approximate the surface of the shell element by calculating the coordinates of any point in the shell as bilinear function of the coordinates at the 4 (or 3) nodal points :

$$
\begin{pmatrix} x \\ y \\ z \end{pmatrix} = N_1 \begin{pmatrix} x_1 \\ y_1 \\ z_1 \end{pmatrix} + N_2 \begin{pmatrix} x_2 \\ y_2 \\ z_2 \end{pmatrix} + N_3 \begin{pmatrix} x_3 \\ y_3 \\ z_3 \end{pmatrix} + N_4 \begin{pmatrix} x_4 \\ y_4 \\ z_4 \end{pmatrix}
$$

$$
\begin{aligned}
N_1 &= a_1 + b_1 x + c_1 y + d_1 xy \\
N_2 &= a_2 + b_2 x + c_2 y + d_2 xy \\
N_3 &= a_3 + b_3 x + c_3 y + d_3 xy \\
N_4 &= a_4 + b_4 x + c_4 y + d_4 xy
\end{aligned}
$$

15

The midsurface of the shell is thus approximated over the element by an 'as flat as possible' surface

- The interpolation functions have identical values in a physical point of the element, independently of the coordinate system

The 16 coefficients can be determined from expressing the trivial condition that each interpollation function has a value of 1 in the corresponding nodal point and zero in the three others :

	N1	N2	N3	N4
x1-y1	1	0	0	0
x2-y2	0	1	0	0
x3-y3	0	0	1	0
x4-y4	0	0	0	1

For a general (trapezoidal, warped) element, this is not trivial and usually the interpolation functions are determined in the isoparametric coordinate system since the interpolation formulas must hold in any coordinate system :
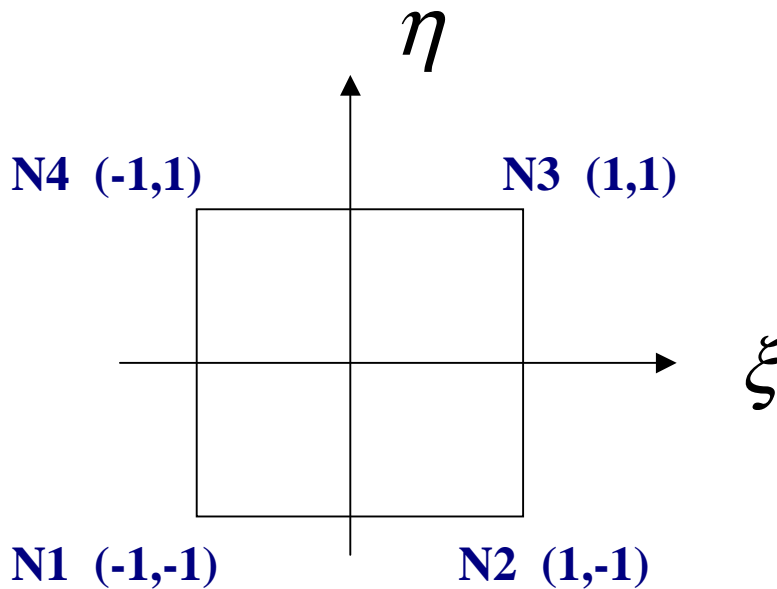
In the isoparametric system the interpolation functions are trivially determined in their more familiar form :

$$N_1 = \frac{1}{4}(1-\xi)(1-\eta)$$

$$N_2 = \frac{1}{4}(1+\xi)(1-\eta)$$

$$N_3 = \frac{1}{4}(1+\xi)(1+\eta)$$

$$N_4 = \frac{1}{4}(1-\xi)(1+\eta)$$

In the element center we thus have :

$$\xi = \eta = 0$$

$$N_1 = N_2 = N_3 = N_4 = \frac{1}{4}$$

$$\frac{\partial N_1}{\partial \xi} = -\frac{1}{4} \qquad\qquad \frac{\partial N_1}{\partial \eta} = -\frac{1}{4}$$

$$\frac{\partial N_2}{\partial \xi} = \frac{1}{4} \qquad\qquad \frac{\partial N_2}{\partial \eta} = -\frac{1}{4}$$

$$\frac{\partial N_3}{\partial \xi} = \frac{1}{4} \qquad\qquad \frac{\partial N_3}{\partial \eta} = \frac{1}{4}$$

$$\frac{\partial N_4}{\partial \xi} = -\frac{1}{4} \qquad\qquad \frac{\partial N_4}{\partial \eta} = \frac{1}{4}$$

Local coordinate systems :

- All operations needed to treat the shell element are performed in a local coordinate system that is called local, or corotational system for MR and CBR shells

- strains, strain rates and stresses are typically only expressed in this system

- In a small displacement context, this system is determined once at the first cycle and corresponds to the undeformed configuration of the shell element

- In a large displacement context (LS-DYNA) the local system must be recomputed every cycle and is based on the current geometry of the shell element

- This local system is assumed to be stationary in space at every cycle, it is not convected and has no velocity

- The default version of the local system in LS-DYNA is dependent upon the node numbering of the element : it follows the global rotation of the element side N1N2, this is irrelevant only if the element shear deformations remain small

- The local z-axis is determined as the vector product of the 2 element diagonals :
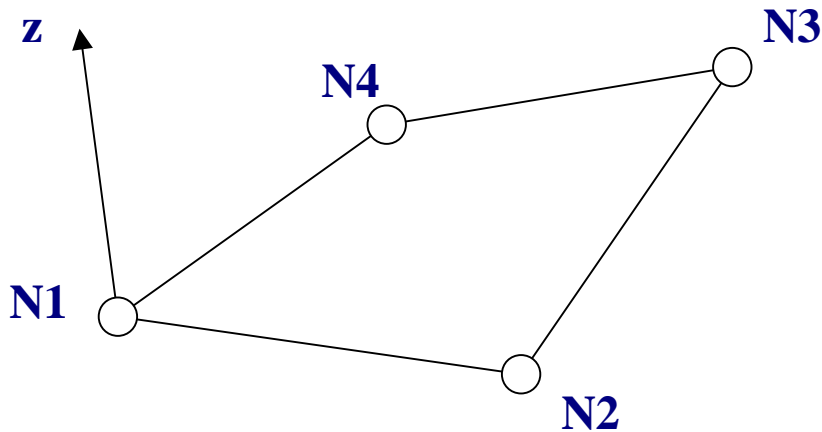
- As seen the origin for the local system is chosen in the first element node N1

- The local z-axis is determined as :

$$\vec{e}_z = \frac{\overrightarrow{N1N3} \times \overrightarrow{N2N4}}{\left\| \overrightarrow{N1N3} \times \overrightarrow{N2N4} \right\|}$$

- The local x-axis is then positioned as well as possible along the element side N1-N2, the match will only be exact if the element is flat :
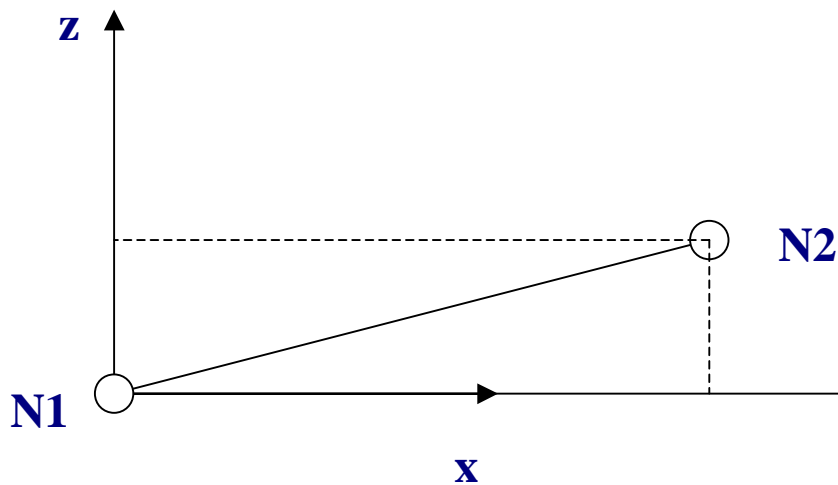
- The local x- and y-axes are then determined as :

$$\vec{e}_x = \frac{\overrightarrow{N1N2} - \left(\overrightarrow{N1N2} \bullet \vec{e}_z \right) \vec{e}_z}{\left\| \overrightarrow{N1N2} - \left(\overrightarrow{N1N2} \bullet \vec{e}_z \right) \vec{e}_z \right\|}$$

$$\vec{e}_y = \vec{e}_z \times \vec{e}_x$$

This simple procedure defines an orthonormal local coordinate system for every configuration of the shell element

- All vectorial quantities (velocities, coordinates) will be transformed in the local system in order to calculate strain rates and stresses in the shell

- This is done using the orthogonal transformation matrix

$$\vec{\vec{Q}} = \begin{pmatrix} \vec{e}_x & \vec{e}_y & \vec{e}_z \end{pmatrix}$$

$$\vec{\vec{Q}}^T = \begin{pmatrix} \vec{e}_x^T \\ \vec{e}_y^T \\ \vec{e}_z^T \end{pmatrix} = \vec{\vec{Q}}^{-1}$$

- The transformations are trivial and correspond to the projection of global vectors on local base vectors :

$$\hat{\vec{x}} = \vec{\vec{Q}}^T \vec{x}$$

$$\hat{\dot{\vec{x}}} = \vec{\vec{Q}}^T \dot{\vec{x}}$$

$$\hat{\dot{\vec{\vartheta}}} = \vec{\vec{Q}}^T \dot{\vec{\vartheta}}$$

- Note : in these notes we usually do not use the hat-notation since all equations are expressed in the local element system

- The definition of the local reference system is somewhat arbitrary since the x-axis is placed along the N1N2 side, this means there is a preferred direction in the element that depends upon the nodal numbering

- This leads to problems if shear deformations are large

20

- In LS940 and higher, a different , node invariant formulation of the local system can be selected that will considerably improve numerical stability if in-plane shear deformations occur in the shell

- This formulation prevents non-physical rotations of the stress tensor and thus improves overall stability and prevents hourglass modes from developing

- This is selected by setting INN=2
  on the CONTROL_ACCURACY card

- This option is available for all shell formulations that use a local reference system

- All shell elements use a local reference system, except types 1 and 6 (original Hughes-Liu)

PAUL A. DU BOIS: **e-mail: paul.dubois@gmx.net**

Consulting Engineer:
> Paul A. Du Bois has been a consultant to the automotive industry since September of 1987. His primary field of activity is large scale finite element simulations for crashworthiness engineering problems. He also conducts advanced engineering software training classes. He is fluent in Dutch, German, French and English

---

* *

Benefits of SGI^{TM} Origin® 300 Technology for MCAE Applications
                    Courtesy of: Stan Posey
                SGI, Director, Manufacturing Industry Development

The application of mechanical computer-aided engineering (MCAE) provides essential tools for efficient design of products and processes. Industries such as automotive, aerospace, and a variety of general manufacturers benefit from MCAE applications that enable reduced design cycle time and costs and improved design quality.

MCAE applications extend the geometry-definition capabilities of mechanical computer-aided design software and offer methods for evaluation of a design's functional behavior under "in-operation" conditions. This is accomplished through application of numerically intensive MCAE software with high-performance computing (HPC) system technology.

This article examines the benefits of a new HPC server, SGI Origin 300, which was developed to advance current capabilities of technical HPC, including MCAE applications.

Introduction

The combination of MCAE application software and HPC system technology provides engineers with an increasingly competitive advantage in today's global manufacturing industry. MCAE applications assist engineers with predictions of design function and performance by simulation of the mechanical loads applied during a design's operation. Examples of these are thermal and mechanical stress, vibration, impact loads, and fluid induced pressure, among others. This variety of load conditions gives rise to design complexities and trade-offs when target objectives for product safety, fuel economy, environmental impact, and consumer appeal are considered, with attempts to reduce time-to-market and increase competitiveness.

Developments in HPC and visualization technology continue to rapidly advance MCAE simulation capabilities of engineers globally. SGI is an established leading supplier of this technology with the company's SGI^{TM} Origin® and SGI^{TM} Onyx® product families. Evidence of SGI success was reported in a recent study issued by D. H. Brown & Associates entitled Symmetric Multiprocessing Dominates High-Performance Computing in CAE, which concluded that SGI was the platform of choice of respondents. This conclusion is consistent with similar industry views that include most of MCAE software providers, who acknowledge SGI as their most strategic hardware partner.

Success with MCAE applications is the result of SGI's ability to offer a scalable SGI^{TM} Origin® 3800 single-system image (SSI) with up to 512 processors and 1TB of single address space (SAS) memory, pushing MCAE simulations to achievements of a historic level. At the core of this remarkable capability is a scalable IRIX® operating system and the cache coherent SGI^{TM} NUMA (nonuniform memory access) system architecture. These HPC technologies combine to offer industry and manufacturing research organizations a high-

availability, nondegrading, and efficient application environment that ensures turnaround and throughput are delivered in support of hundreds of simultaneous users with a demanding mix of MCAE applications.

SGI continues to invest in the MCAE community's shared vision and success with introduction of SGI Origin 300, an HPC server that enables further advancements for MCAE applications. SGI Origin 300 delivers the existing application advantages of IRIX and NUMA with complete SGI^{TM} Origin® 3000 series compatibility, yet in a package that is significantly smaller than a similar SGI Origin 3000 series configuration. While the SGI Origin 3000 series offers large-scale data center HPC, SGI Origin 300 scales from 2 to 32 processors and offers a midrange HPC solution as either a departmental SSI server or a large HPC cluster of these servers.

HPC Characteristics of MCAE Software

From a hardware and MCAE software algorithm perspective, there are roughly three types of MCAE application disciplines to consider: implicit and explicit finite element analyses (FEA) for structural analysis and computational fluid dynamics (CFD) for fluid flow simulation. There is further segmentation of implicit FEA since structures (and associated algorithms) at rest (static) and those in motion (dynamic) behave differently. This gives rise to four distinct types of MCAE software application behavior.

Generally speaking, MCAE software applications exhibit a range of various HPC resource demands for each of the four segments described. An examination of these demands aids in a proper characterization of what features are required from an effective HPC system architecture. For example, the desired features for MCAE from a RISC system architecture include fast processors with a Level 2 cache, large addressable memory, high memory-to-processor bandwidth rates, high disk-to-memory I/O rates, and a low-latency interconnect that provides efficient parallel scalability to hundreds of processors.

A closer examination of the different demands from each of the four segments highlights the importance of a balanced HPC system architecture. For example, implicit FEA for static load conditions requires a fast processor for effective turn-around, in contrast to dynamic response, which requires high rates of memory and I/O bandwidth with processor speed as a secondary concern. In addition, FEA modeling parameters such as the size, the type of elements, and the load condition of interest all affect the resulting execution behavior of implicit and explicit FEA applications.

Explicit FEA benefits from a balance of fast processors for the required element force calculations and high rates of memory bandwidth necessary for the efficient contact resolution that is required for nearly every structural impact simulation. CFD also requires a balance of memory bandwidth and fast processors, but benefits most from parallel scalability. Each segment has inherent complexities with regard to efficient parallel scaling, depending upon the particular parallel scheme and system architecture. While CFD scales efficiently to hundreds of processors, explicit FEA scales to 50 and implicit FEA to less than 10.

A system architecture that can achieve high parallel efficiency becomes increasingly important as algorithms for MCAE software applications have developed such capability. Most commercial MCAE software employs a distributed memory parallel (DMP) technique for compatibility across the range of RISC architectures available. Other techniques include shared memory parallel (SMP) and hybrid parallel schemes that take advantage of both DMP and SMP within a single computation. The scalability of SMP algorithms is limited to the number of processors offered in an SSI, meaning scaling beyond the maximum 32 processors of an SGI Origin 300 server would require implementation of a DMP technique.

Most MCAE software is carefully designed to avoid major sources of parallel inefficiencies, whereby communication overhead is minimized and proper load balance is achieved. For MCAE software that utilizes a DMP technique with a message passing library such as MPI, development of an SGI NUMA-aware MPI is included for MCAE software and is transparent to the user. This MPI further reduces communication overhead when scaling to a large number of processors, which is achieved by a reduction in latency that is more than threefold improved over public domain MPICH.

SGI Origin 300 System Technology for MCAE

The SGI Origin family has a NUMA multiprocessor architecture that is a breakthrough implementation of conventional SMP architectures. The SGI NUMA architecture distributes memory to individual processors in order to reduce latencies that inhibit high bandwidth and scalability. At the same time, all memory is globally addressable to enable high-resolution MCAE modeling and simplify MCAE algorithm development. A single image SGI Origin 3800 system offers the largest SMP system currently available.

The SGI NUMA architecture was introduced in the SGI Origin 2000 server in 1995, and later advanced with the SGI^{TM} NUMAflex^{TM} modular design concept of the SGI Origin 3000 series. Now the same high bandwidth and low latency NUMA architecture is available in SGI Origin 300, yet with a significant cost-performance advantage for MCAE applications. This is achieved, amongst others, by reducing the size of Level 2 cache of the MIPS® processor from 8MB to 2MB, while keeping the performance penalty limited to 15%, even with the most cache-intensive MCAE applications.

The modular building block of the SGI Origin 300 system is a node that contains two or four MIPS processors, corresponding memory up to 4GB, and a connection to a portion of an I/O subsystem. The hub interface to the node is the distributed memory controller, and nodes are connected together via the NUMAlink^{TM} cable or module in a maximum SSI configuration of 32 processors that requires only half a rack. Alternatively, these same node modules can be clustered with a choice of scalable interconnect networks to much larger processor counts and system configurations.

Conclusions

A discussion was provided on the HPC technology requirements of MCAE applications, including characterizations of the performance behavior typical of four types of conventional MCAE simulations. The HPC technology offered with the new midrange SGI Origin 300 server is well-suited to the demands of each MCAE application segment. In particular, the choice offered with SGI Origin 300 as a moderately configured SSI for departmental deployment, or as a large cluster for scalable DMP applications, provides substantial performance benefits to MCAE applications for a range of modeling requirements.
SGI Origin 300 design breakthroughs in cost-effectiveness and compact packaging will further expand the use of MCAE and HPC to include a variety of applications in the mainstream of product and process development. With SGI Origin 300, the entire suite of MCAE applications can now achieve capability levels that are nearly equivalent to the industry-leading SGI Origin 3000 series up to 32 processors, but at roughly half the cost. This new SGI technology development for the MCAE community demonstrates the company's continued commitment to delivering valuable leadership to the manufacturing industry.

sgi

Theme Engineering Inc. sponsored the 6th LS-DYNA Users Conference in Seoul, Korea on November 5th, 2001.   Approximately 8 excellent technical presentations were given with about 100 engineer, researchers participating in the conference.

THEME would like to give special thanks to Dr. John Hallquist and Mr. Arthur Tang for their excellent presentations.

Dr. Junghoon Chung from KIMM was awarded the prize for the best paper submitted.

We hope you will all join us for our next conference.

 THEME Engineering, Inc.

Suite 409 Daeryung B/D 327-24, Kasan-dong, Kumchun-ku,
Seoul, 153-023, KOREA
Tel : 82-2-839-5804~7
Fax : 82-2-839-5860
URL : www.theme-eng.co.kr (www.lsdyna.co.kr)
E-mail : theme@soback.kornet.net

FEA Information

Geomaterial Modeling

www.geomaterialmodeling.com

Geomaterials, which include soil, rock, and concrete are common building materials for civil and defense structures.

Soil and rock are natural materials, often used to support or embed structures. Examples of the use of soil and rock:

- civil construction foundations rest on soil or rock.
- tunnel structures pass through soil and rock.
- in defense applications, soil and rock are often used to hide installations and strong rock types can act as a protective barrier.

Concrete, especially reinforced concrete, is a widely used construction material in both civil and defense applications. The low cost, and easy formability of concrete, often makes it the optimum material for construction. The range of physical sizes of concrete structures run from a simple concrete storage pad to the largest dam construction project in the world being carried out in China.

Strength Characteristics: Geomaterials span a wide range from relatively weak sands to one of nature's strongest material, granite. Although these two geomaterials span a wide strength range, their constitutive response characteristics are relatively similar; although very different from more familiar common metal constitutive responses.

Page 2: Constitutive Modeling - Figure 1 (Axial Compression of a reinforced concrete column.)
Page 3: Recommended Reading

Information for our Geomaterial Modeling site is provided courtesy of Len Schwer, Ph.D., Schwer Engineering & Consulting Services. Dr. Schwer teaches a course Geomaterial Modeling with LS-DYNA

Events: if you have an event you would like to list contact mv@feainformation.com

2002	Company	Event
April 08-10 France	**MSC**	Worldwide Aerospace Conference & Technology Showcase, Toulouse, France
April 22-24 USA	**ANSYS Inc.**	ANSYS Users Conference & Exhibition 2002 - Pittsburgh Hilton, Pittsburgh, PA. For information visit:
May 19-21, USA	**LSTC ETA**	7th International LS-DYNA User's Conference at the Hyatt Regency Hotel & Conference Center - Fairlane Town Center, Dearborn, MI 48126
Oct. 9-11 Germany	**CAD-FEM**	CAD-FEM Users Meeting - International Congress on FEM Technology: Kultur- und Congress-Centrum "Graf-Zeppelin-Haus", Friedrichshafen, Lake Constance, Germany. For information contact Barbara Leichtenstern. Information will be available soon on the CAD-FEM website

FEA Information contributing sponsors
dedicated to worldwide engineering information, sales, training, consulting

Headquarters	Company	website
Australia	Leading Engineering Analysis Providers	www.leapaust.com.au
Belgium	LMS, International	www.lmsintl.com
Canada	Metal Forming Analysis Corp.	www.mfac.com
China	ANSYS Bejing	www.ansys.com (link on international)
France	Dynalis	www.dynalis.fr
India	GissEta	www.gisseta.com
Japan	The Japan Research Institute, Ltd	www.jri.co.jp
Japan	Fujitsu Ltd.	www.fujitsu.com
Korea	THEME Engineering	www.lsdyna.co.kr
Korea	Korean Simulation Technologies	www.kostech.co.kr
Russia	State Unitary Enterprise - STRELA	www.ls-dynarussia.com
Sweden	Engineering Research AB	www.erab.se
Taiwan	Flotrend Corporation	www.flotrend.tw
UK	OASYS, Ltd	www.arup.com /dyna
USA	Livermore Software Technology	www.lstc.com
USA	Engineering Technology Associates	www.eta.com
USA	ANSYS, Inc	www.ansys.com
USA	Hewlett Packard	www.hp.com
USA	SGI	www.sgi.com
USA	MSC Software	www.msc.com
USA	EASi Engineering	www.easiusa.com
USA	DYNAMAX	www.dynamax-inc.com

FEA Information News Showcased in November
Archived on the site on the News Page

November 5th

Software:	**MSC**	MSC.PATRAN
Software:	**JRI**	JMAG
Distributor:	**LEAP**	Located in Australia

November 12th

Hardware:	**SGI**	Origin 300 server
Software:	**Oasys**	Primer
Distributor:	**MFAC**	Located in Canada

November 19th

Hardware:	**HP**	Workstation X4000 Linux
Software:	**ANSYS**	Design Space
Distributor:	**DYNAMAX**	Located in USA

November 26th

Software:	**EASi**	EASi-Process
Hardware:	**Fujitsu**	Primepower
Distributor:	**ERAB**	Located in Sweden

FEA Information Educational Participants

Dr. T. Belytschko Northwestern U. USA	**Dr. D. Benson** UCSD USA	**Dr. Bhavin V. Mehta** Ohio University USA
Dr. Taylan Altan The Ohio State U. ERC/NSM USA	**Prof. Ala Tabiei** U. of Cincinnati USA	**Dr. Alexey I. Borovkov** St. Petersburg State Technical. University Russia

December Participant Showcase

STRELA russia

http://www.ls-dynarussia.com

State Unitary Enterprise – STRELA, RUSSIA
Alexey Abramov
Olga Voikina

4560770, Snezhinsk, Chelybinsk Region
Vasilyeva St. 13, U1, Russia
e-mail: lsdyna@strela.snz.ru

FEA Information Showcase
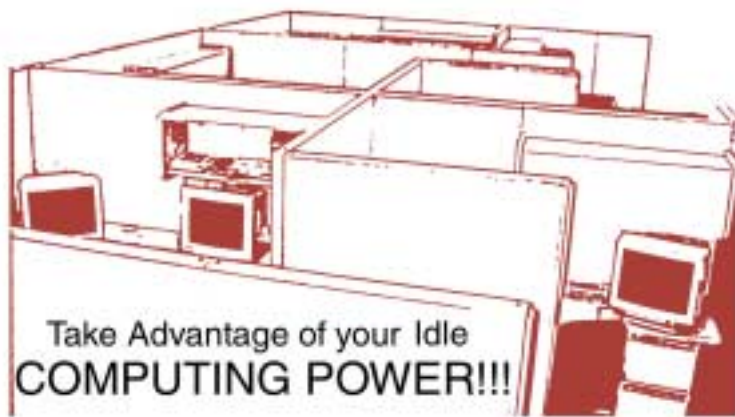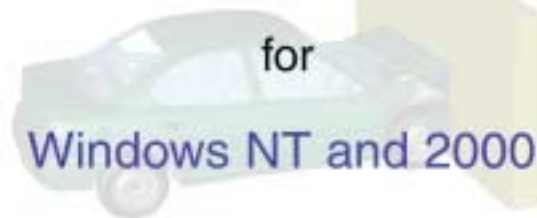
Livermore Software Technology Corporation
[www.ls-dyna.com]
[www.lstc.com]

For More Information on Availability

Contact: Wayne L. Mindle
wlm@lstc.com

Take Advantage of your Idle COMPUTING POWER!!!

LS-DYNA MPP for **Windows NT and 2000**

The Japan Research Institute Limited
www.jri.co.jp
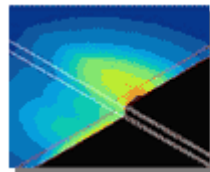
JMAG-Studio

Electromagnetic Wave Analysis

Applications:
  Antennas, Electronic Devices, PCBs, Strip Lines, EMC, Wave Absorbers, Electromagnetic Shields, Waveguides, Resonators, Plasma, Optical Pickups, Magneto-Optical Recording, Cellular Phones, Microwave Ovens

Features:

- Analysis selectable either in the frequency domain (Finite Element Method) or the time domain (Finite Difference Time Domain) depending on the problem.

- Both dielectric and magnetic material properties may be frequency dependent.

- Coupled thermal analysis

For Complete Information on JMAG-Studio: **http://www.jri.co.jp/pro-eng/jmag/e/jmg/index.html**

Product names referred herein are trademarks of their respective companies